Hindawi
International Journal of Antennas and Propagation
Volume 2022, Article ID 3883786, 12 pages
https://doi.org/10.1155/2022/3883786

Research Article

Low-Cost Lens Antenna Design for Microwave Moisture Detection

Fangyan Ma, Xinpei Zhang, Yuanyuan Yin, Hang Yin, Chao Song, and Liqing Zhao

College of Mechanical and Electrical Engineering, Qingdao Agricultural University, Qingdao 266109, China

Correspondence should be addressed to Liqing Zhao; liqingzhao611@163.com

Received 26 May 2022; Revised 5 July 2022; Accepted 3 August 2022; Published 28 August 2022

Academic Editor: Shah Nawaz Burokur

In this study, a novel Vivaldi antenna with dimensions of 100 mm × 85 mm × 1.6 mm, designed for a moisture measurement system, is built to enhance the gain of conventional Vivaldi antennas in the low-frequency band to suit the needs of moisture detection. The fence structure and choke slot are modified to enhance the antenna's radiation properties in the low-frequency band, and simulation is performed to determine how different structural parameters affect the antenna's performance. The results show that in the frequency band of 5-6 GHz, the voltage standing-wave ratio (VSWR) of the antenna is less than 2, and the gain at 5.8 GHz reaches 16.2 dBi after installing the lens. Compared with conventional unmodified Vivaldi antennas, the gain at 5.8 GHz increases by approximately 6.11 dBi. The antenna is then processed and measured, and the measured results are in good agreement with the simulated results; hence, the antenna can be widely used in the field of moisture detection.

1. Introduction

Online measurement of moisture has become an urgent problem to be solved in the field of food production [1, 2]. The development of moisture sensors based on the microwave free-space method is presently a popular research direction. The main principle of this method is to calculate the moisture in the material by measuring the loss caused by the polarization of water when microwaves pass through the material; the main parameters that change owing to loss are S_{21} and S_{11}, so the dielectric properties of the material can be calculated from these two parameters, and the electric constant can be used to further calculate the moisture content of the material. As part of the sensor, the antenna plays an important role in the measurement of S_{21} and S_{11}. Trabelsi et al. [3] developed, calibrated, and tested a microwave moisture meter—made of off-the-shelf components—in the laboratory and field in 2016 in the examination of in-shell peanuts by measuring the dielectric properties of peanut pod samples. To achieve nondestructive and instantaneous determination of kernel moisture content, the device uses a flat-panel antenna, which makes the whole device larger and limits portability.

The Vivaldi antenna is developed as an ultrawideband antenna with a directive pattern and high gain, which is attractive for radar application and microwave sensing [4]. When the antenna is operational, the electromagnetic wave guided by the exponential slot line realized on the front metal layer excited by a lower microstrip line is radiated into free-space [5]. Lin et al. [6] designed an asymmetric wideband dual-polarized bilateral tapered-slot antenna for wireless measurement of electromagnetic compatibility. This antenna has achieved good results. Nevertheless, compared to the planar structure previously described, its three-dimensional structure takes up even more space. Teni et al. [7] designed a novel miniaturized antipodal Vivaldi antenna with improved radiation characteristics. It performs relatively well in all aspects except for the gain which does not meet the requirements of the standard moisture sensor, making it unsuitable for this application.

Selecting the appropriate type of antenna and rationally optimizing its size and shape can achieve good antenna radiation characteristics so that the antenna has high gain, low VSWR, low return loss, sharp main lobe, and small side lobes. Furthermore, the ideal design can compress device volume, improve portability, and reduce cost [8–10]. Compared with the traditional horn antenna, the Vivaldi antenna has a unidirectional and stable radiation pattern and has a simpler structure, easier processing, and lower cost. Its

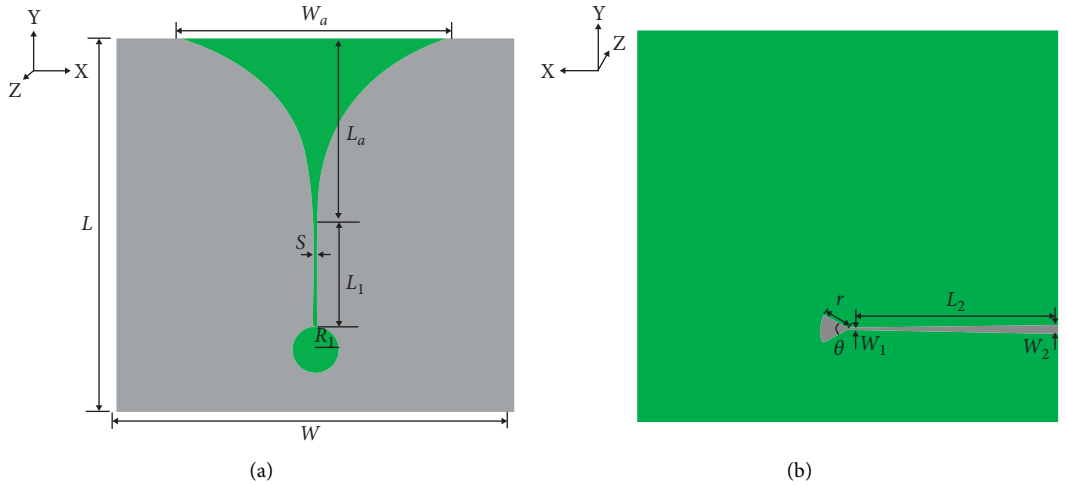

Figure 1: Structure of conventional Vivaldi antennas: (a) front; (b) back.

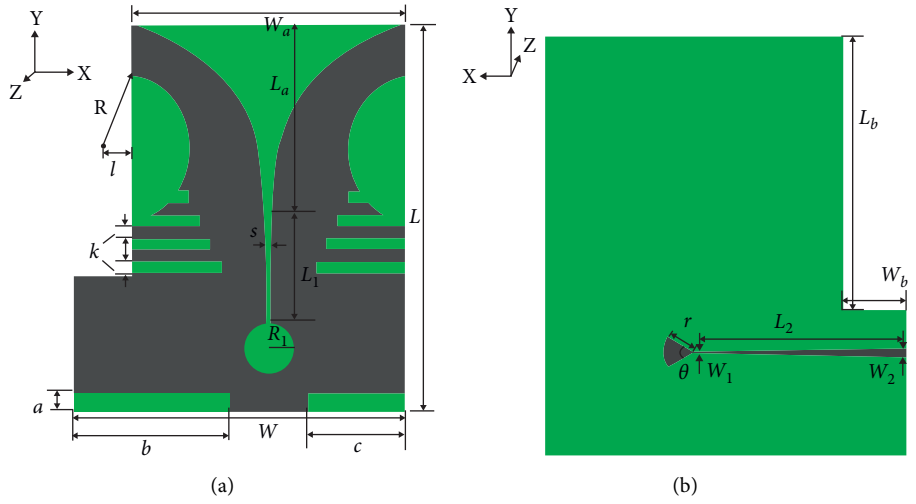

Figure 2: Structure of improved Vivaldi antenna: (a) front; (b) back.

lens can convert spherical waves into plane waves, concentrating the radiation energy and narrowing the beam [11] to improve contact with the measured object. Therefore, a low-cost lens Vivaldi antenna, for grain microwave moisture detectors, is presented in this paper. The full-wave software CST Microwave Studio was employed to analyze and design the antenna. Finally, an antenna prototype was realized to verify the fulfillment of the design requirements.

2. Parametric Design

2.1. Vivaldi Antenna Design. The Vivaldi antenna covers the two sides of the dielectric plate with a metal layer. The antenna is mainly composed of three parts a circular cavity, a slot line followed by an exponential slot line [12], and a microstrip line printed on its backside.

In particular, when the opening of the exponential slot is small, the electromagnetic energy is bound between the two metal arms forming the antenna, so the radiation is weak; while energy emission increases as the electromagnetic field travel along the exponential slot, thus favoring the energy emission into free-space at the antenna opening [13].

Table 1: Antenna parameters.

Parameter	Conventional antennas	Improved antenna
L	100 mm	100 mm
W	105 mm	85 mm
W_a	70 mm	70 mm
W_b	—	15 mm
L_a	49.5 mm	49.5 mm
L_b	—	65 mm
L_1	30 mm	30 mm
R	—	35 mm
l	—	15 mm
S	1 mm	1 mm
R_1	6.5 mm	6.5 mm
r	7.3 mm	7.3 mm
θ	60°	60°
W_1	0.25 mm	0.25 mm
W_2	2 mm	2 mm
L_2	25 mm	25 mm
a	—	5 mm
b	—	42.5 mm
c	—	27.5 mm
k	—	3 mm

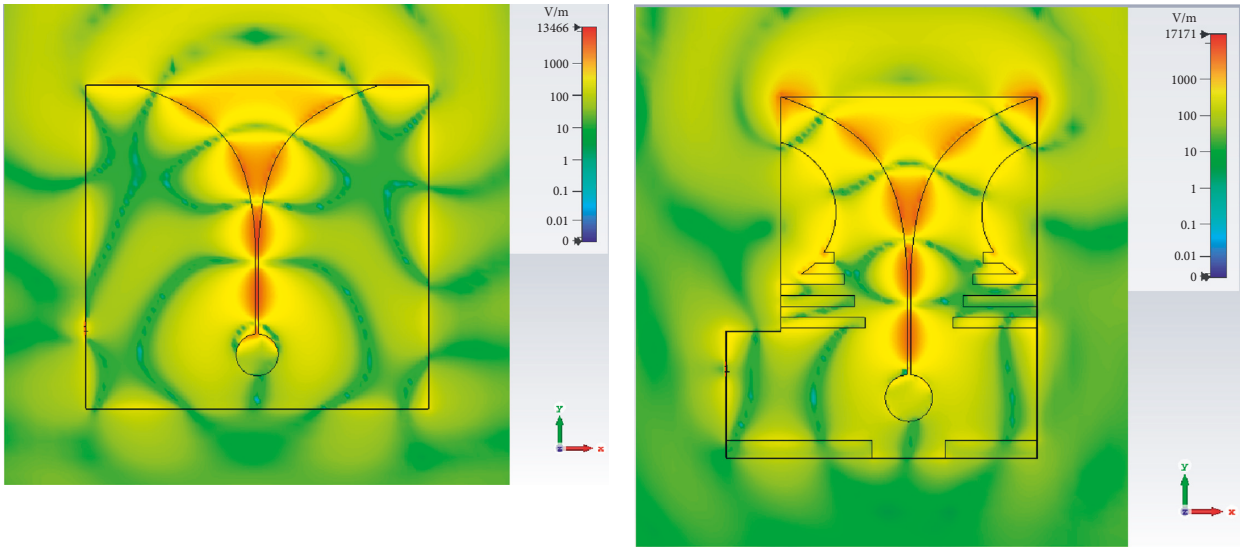

(a) (b)

Figure 3: Transverse components of y-x electric field ($f = 5.8$ GHz): (a) conventional Vivaldi antenna; (b) improved Vivaldi antenna.

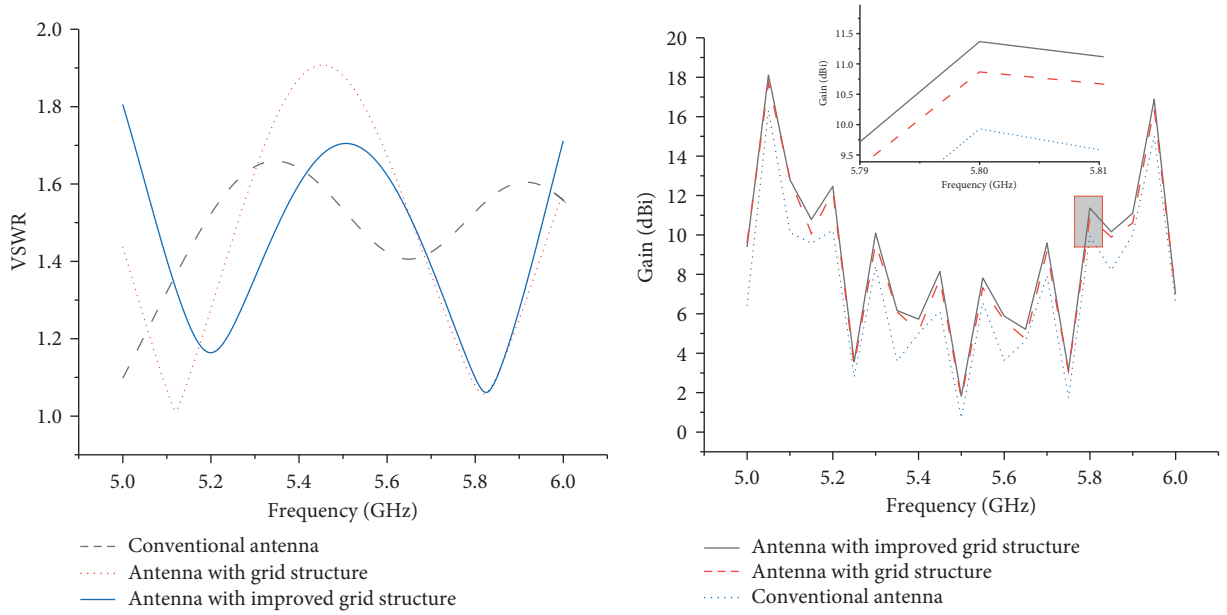

(a) (b)

Figure 4: Performance parameters: (a) voltage standing-wave ratio; (b) gain of antenna.

Therefore, the minimum distance of the exponential slot line of the antenna determines the highest operating frequency of the antenna, whereas the maximum opening size of the slot line limits the lowest operating frequency of the antenna [14–16].

To meet the parameter requirements of the moisture gauge, the performance indicators to be achieved by a modified Vivaldi antenna are preset in this paper. To verify the performance of the proposed moisture sensor we decided to test the system not only at 5.8 GHz but also in the 5-6 GHz band. Therefore, the antenna must be able to operate with a gain greater than 10 dBi at the working frequency, with VSWR not exceeding 2. The designed microstrip antenna consists of a substrate and a patterned copper layer. The substrate material is an FR-4 sheet (dielectric constant is 4.2–4.7, loss tangent is 0.02, and thickness is 1.6 mm). The initial microstrip size can be computed [17] as follows:

$$L = \frac{c}{f_L}\sqrt{\frac{2}{\varepsilon_r + 1}},$$
$$W = \frac{c}{2f_L\sqrt{\varepsilon_r}}. \quad (1)$$

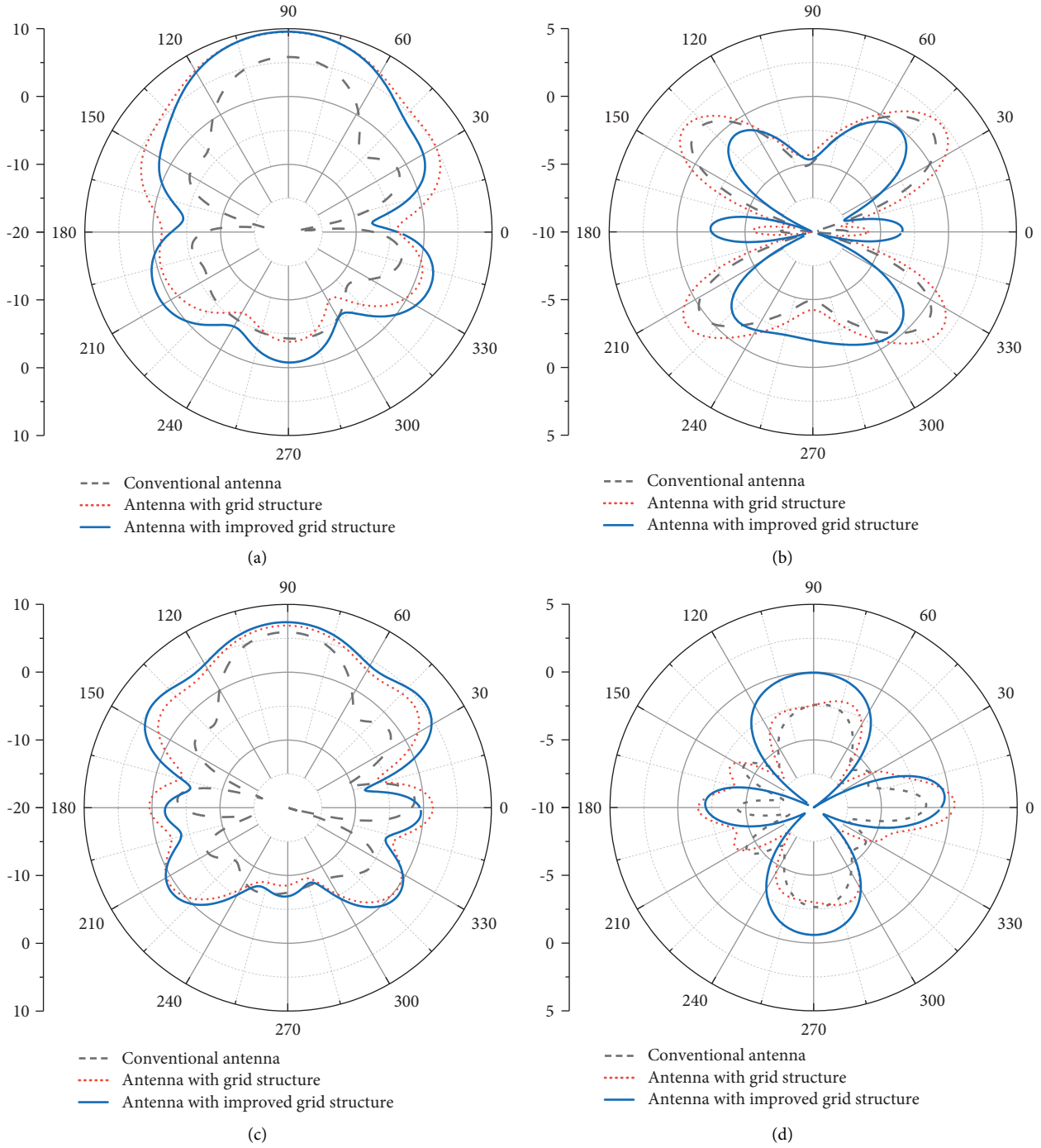

Figure 5: Continued.

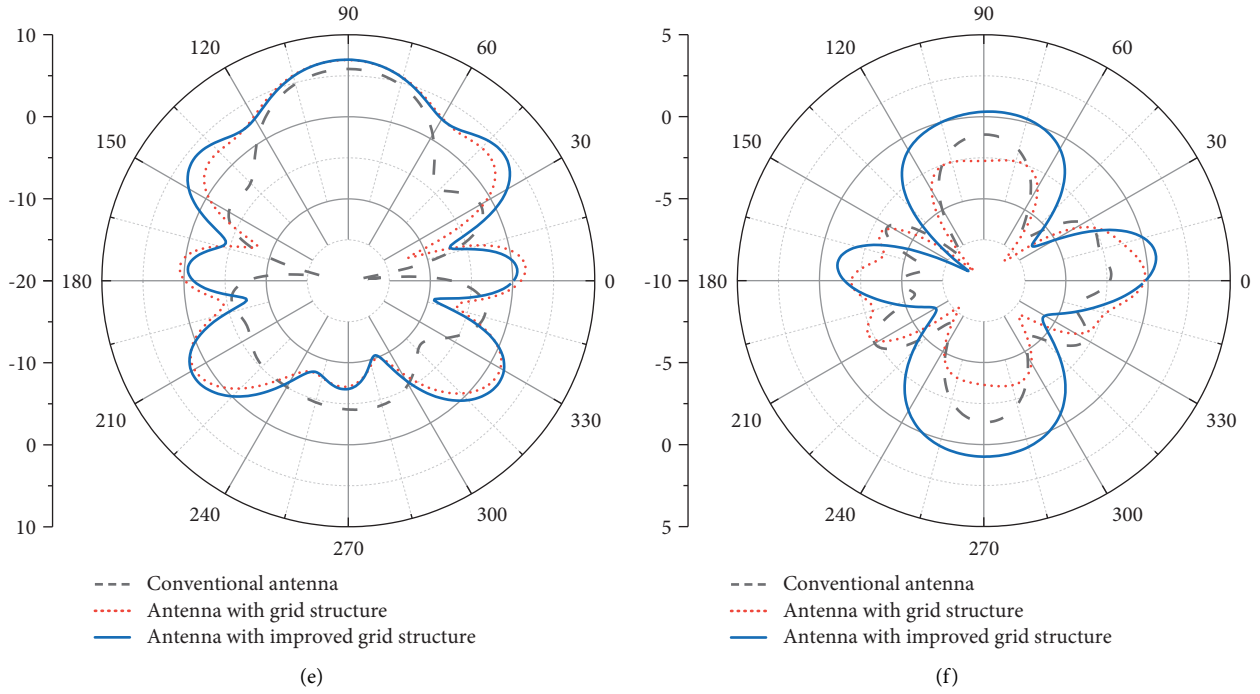

Figure 5: Antenna electric field radiation patterns: (a) *y-z* plane radiation patterns at 5 GHz; (b) *x-y* plane radiation patterns at 5 GHz; (c) *y-z* plane radiation patterns at 5.8 GHz; (d) *x-y* plane radiation patterns at 5.8 GHz; (e) *y-z* plane radiation patterns at 6 GHz; (f) *x-y* plane radiation patterns at 6 GHz.

Table 2: Performance comparison among different antennas.

Reference	Bandwidth (GHz)	Maximum realized gain (dBi)	Antenna size (mm)	Structural complexity	Lens	Application
[1]	2.45	Unknown	140 × 140	Simple	No	Moisture content measuring
[7]	0–30	7	50 × 66.4	Simple	Yes	High dynamic-range imaging
[8]	1.54–7	9.8	88 × 75	Simple	No	Breast phantom measurement
[11]	2–8, 8–40	12.1	130 × 130 × 243	Complex	No	Radio-frequency simulation system
[13]	1.38–13.8	12.6	182 × 96 × 6.1	Simple	No	Communication and radar technologies
[18]	4–40	7.8	80 × 80 × 94	Simple	No	Mobile infrastructure
[19]	4–13	9.2	40 × 4 × 0.8	Complex	No	High dynamic-range imaging
This work	5-6	16.5	100 × 85 × 1.6	Simple	Yes	Moisture content measuring

Here, L is the length of the substrate, W is the width of the substrate, c is the speed of light, f_L is the lowest frequency, and ε_r is the dielectric constant.

The profile of the exponential line can be obtained from the following equations:.

$$y(x) = C \cdot e^{K_a x}, \tag{2}$$

$$C = \frac{s}{2}, \tag{3}$$

$$K_a = \frac{1}{L_a} \ln\left(\frac{W_a}{s}\right). \tag{4}$$

Here, s is the width of the slot line, L_a is the length of the exponential slot line, and W_a is the width of the flared opening, as detailed in Figure 1.

To reduce the main beam opening angle and improve the antenna gain, we have also modified the metal layer. There will be surface and edge currents in the metal areas on both sides of the slot line, which will affect the antenna gain and directivity. To effectively suppress the surface wave on the outer region of the metal arms some grooves are etched near the edge, so to concentrate the current flow along the exponential slot [18–20]. This improves in-band entrance and antenna gain. Pandey et al. [21] made similar improvements to the Vivaldi antenna; that is, etching the fence structure

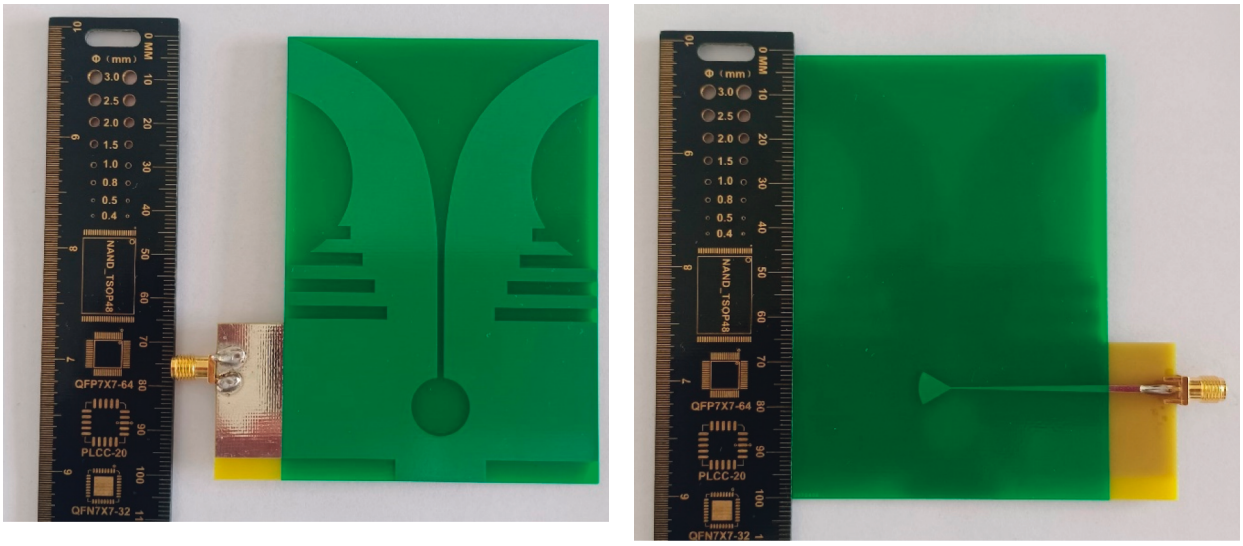

(a) (b)

Figure 6: Antenna prototype: (a) front; (b) back.

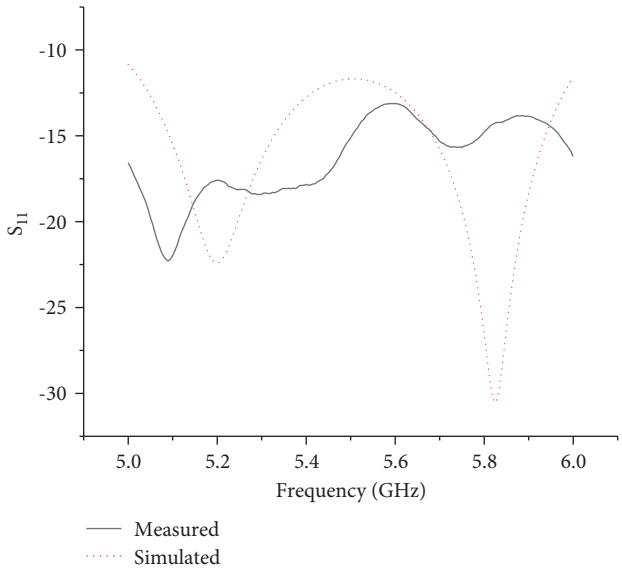

Figure 7: Frequency behavior of antenna reflection coefficient.

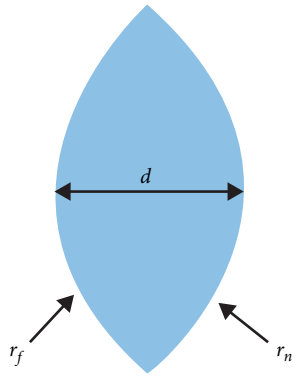

Figure 8: Structure of lens.

Table 3: Spherical lens parameters.

Parameter	Value
D	30 mm
N	1.732
r_f	130 mm
r_n	130 mm
F	93.344 mm

onto the metal layer, and achieved good results. However, we found in the experiment that the gain is greatly improved when the fence structure is further modified. Therefore, in the proposed antenna, we added a grid structure and introduced symmetrical semicircular grooves on both sides of the antenna arms. The modified antenna structure is depicted in Figure 2.

The optimized antenna dimensions are presented in Table 1.

After numerical investigation, the equation of the exponential slot line is expressed as $y(x) = e^{0.08x}$.

The transverse components of the electric field (x and y-components), concerning the antenna before and after the adoption of symmetrical semicircular grooves and grids on both antenna arms, are shown in Figure 3. The map reveals a higher field level in the slot region of the modified antenna as already observed in [20]; the signal level used to excite the improved antenna was 4936 V/m.

At the same time, the related performance parameters of the antenna are obtained by numerical simulation; the standing-wave ratio is shown in Figure 4(a), and the gain is shown in Figure 4(b).

It can be seen from Figure 4 that the conventional Vivaldi antenna has a minimum VSWR of 1.0611 in the frequency range (5-6 GHz), with a maximum of 1.8054, and

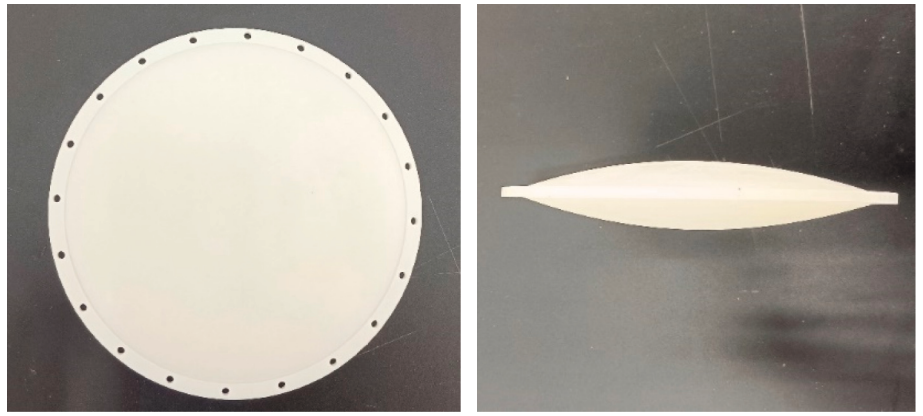

Figure 9: Dielectric lens prototype.

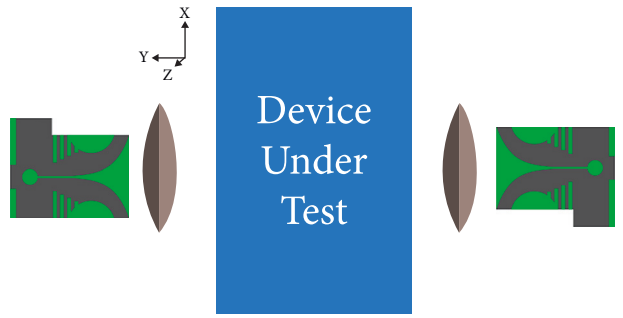

Figure 10: Structure of measuring platform.

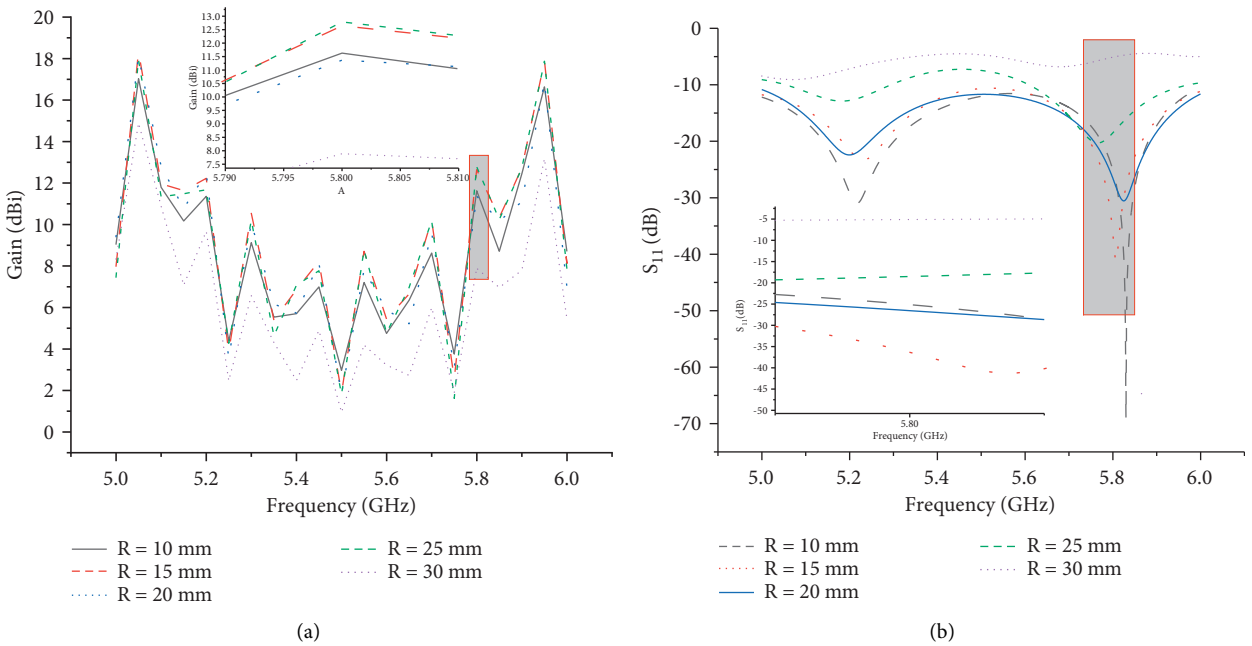

Figure 11: Frequency behavior of the gain (a) and of the magnitude of antenna S-parameter (b) for different values of the curvature radius of the semicircular grooves.

1.0988 at 5.8 GHz. Compared with the VSWR values of the original antenna, the maximum VSWR and the VSWR at 5.8 GHz are both lower and meet the design requirements.

When the improved antenna is at 5.8 GHz, the gain is 11.368 dBi, which is improved compared with the original gain. Although a desirable gain at 5.8 GHz is achieved, it can

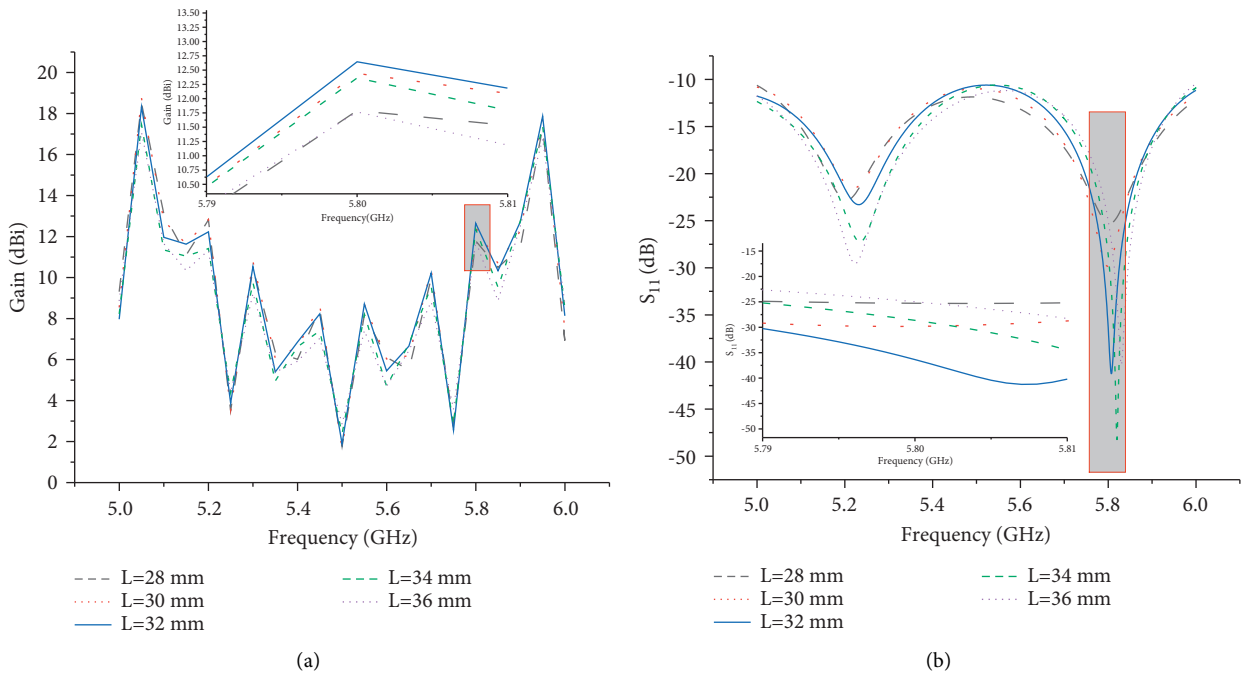

FIGURE 12: Frequency behavior of the gain (a) and of the magnitude of antenna S-parameter (b) for different values of the grooves curvature centers.

nonetheless be seen from Figure 4 that the gain drops significantly at 5.25, 5.5, and 5.75 GHz. By computing the radiation patterns at these frequencies, we found that the main lobe of the antenna was large, so the energy is not focused efficiently, resulting in a decreased gain.

The electric field patterns at different frequencies are shown in Figure 5.

From the analysis of Figure 5 it appears that the opening angle of the antenna beam is 64.2°, 59°, and 47.3° at the frequencies of 5, 5.8, and 6 GHz, respectively, while the radiation angle reduces and the gain increases at 5.8 GHz, thus, satisfying the moisture detection requirements when the antenna is modified. It can be seen from Table 2 that the proposed antenna is the most optimal in terms of relative gain and size.

The improved Vivaldi antenna was then fabricated according to the final design scheme, and its performance was tested. The antenna prototype is shown in Figure 6.

The relative performance of the antenna is evaluated using a vector network analyzer and compared with the simulated performance. The comparison results are plotted in Figure 7.

It can be seen from Figure 7 that although not entirely consistent with the numerical simulation, the frequency behavior of the antenna reflection coefficient still meets the design requirements. The minimum S_{11} is −22.2924 at 5.09 GHz and −14.78981 at the 5.8 GHz operating frequency. These differences may be caused by structural variations resulting from fabrication processes and the performance of raw materials. However, the proposed antenna design meets all the requirements of a microwave moisture sensing system.

2.2. Lens Design. The design of the dielectric lens is based on Fermat's principle and Fresnel's law of refraction [22]. The curve of the lens is designed to convert spherical electromagnetic waves to plane electromagnetic waves. Lens antennas have a unique advantage since they are able to focus the RF energy by significantly increasing the gain in the antenna boresight direction while reducing the level of the side lobes. In this study, two spherical lenses using 9600R photosensitive resin (dielectric constant of 3.5) are designed and placed in front of the transmitting antenna and the receiving antenna, respectively, to process the signal.

The lensmaker's equation [23] is

$$\frac{1}{f} = (n-1)\left(\frac{1}{r_n} - \frac{1}{r_f}\right) + \frac{(n-1)^2 d}{n r_n r_f}, \tag{5}$$

where f is the focal length, n is the refractive index, r_n and r_f are the curvature radius of the lens's rear and front surface, respectively, while d is the thickness of the lens shown in Figure 8.

The lens design parameters are shown in Table 3. The actual dielectric lens is shown in Figure 9.

The distance between the two antennas is 560 mm, and to ensure that the transmitted signal is refracted into a plane wave, and the signal is refocused after the plane wave passes through the target to the receiver, the starting point of the exponential slot line should be placed near the focal point of the lens, so the lens is placed 43.8 mm away from the antenna port. The target to be measured is positioned between the two lenses. The overall configuration is shown in Figure 10.

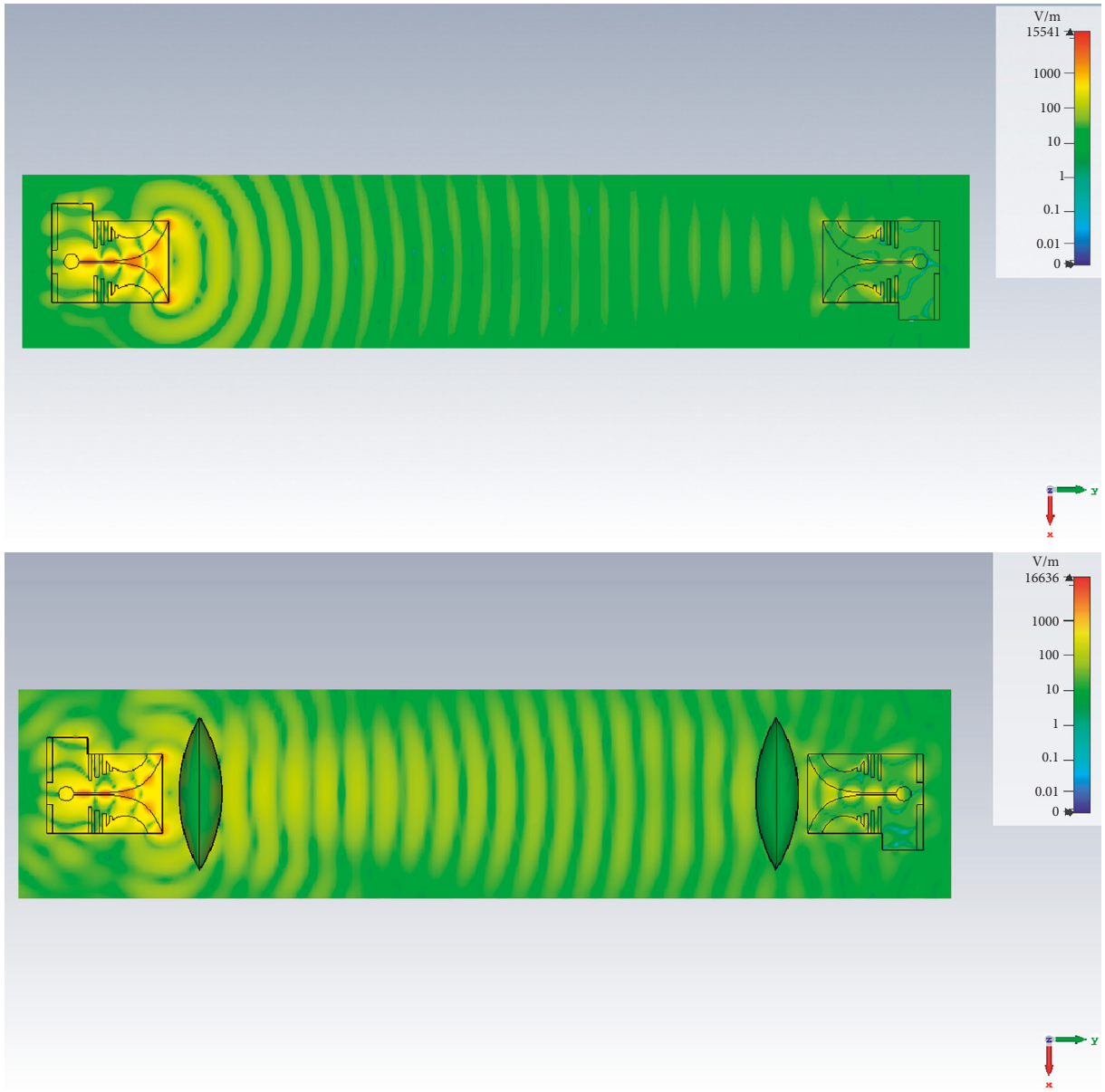

Figure 13: Transceiver system consisting of two Vivaldi antennas without and with dielectric lenses. The field maps concerning the transverse x- and y-components of the electric field were obtained by full-wave numerical simulations at 5.8 GHz.

3. Effects of Improved Structural Parameters on Antenna Performance

The antenna proposed in this study improves the performance of a conventional Vivaldi antenna by optimizing the fence structure and adding a dielectric lens to achieve better radiative performance. To further explore the effect of improving the fence structure and lens on the Vivaldi antenna, we redesigned the antenna by adjusting the positions and radii of its semicircular structure and compared the effect of the lens on the antenna performance parameters.

3.1. Influence of Semicircle Radius on Antenna Performance. Since the curvature radii of the semicircle grooves made on the radiating arms have an impact on the antenna band and gain, a specific investigation was carried out by keeping the centers of the grooves fixed while modifying their curvature radii. In particular, the S-parameters and the antenna gain corresponding to the grooves curvature radii of 30 mm, 25 mm, 20 mm, 15 mm, and 10 mm, were analyzed.

The related performance parameters of the antenna are obtained through numerical simulation: the gain measurement results are shown in Figure 11(a), while the S-parameter measurements are displayed in Figure 11(b).

It can be seen from Figure 11 that when the frequency is 5.8 GHz, the maximum gain is 12.7884 dBi when the semicircle radius is 25 mm; the minimum gain is 7.8898 dBi when the radius is 30 mm, and the gain is 11.368 dBi when the radius is 20 mm (initial design). When the radius is 25 mm, the antenna gain improves with respect to the gain obtained adopting other groove radii, whereas when the

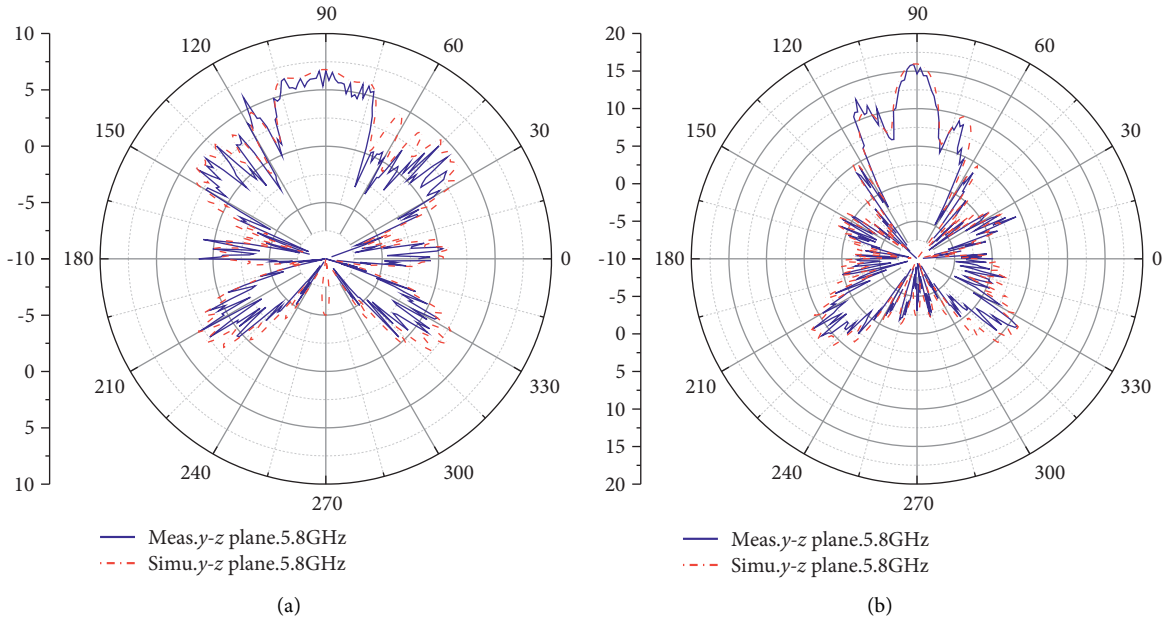

Figure 14: Antenna radiation patterns without (a) and with (b) dielectric lens. A good agreement between numerical simulations and measurements is observed.

radius is 30 mm, the fence structure loses its field focusing characteristics, resulting in a significant decrease in gain.

When the antenna is at 5.8 GHz with the semicircle radius of 25 mm, S_{11} is −18.5141; when the radius is 15 mm, S_{11} is −36.3549, which is the lowest; when the radius is 30 mm, S_{11} is −5.1081, which is the highest; and when the radius is 20 mm (initial design), S_{11} is −26.5457.

Furthermore, at a 15-mm radius, the gain is 12.6451 dBi. Although the gain at this radius is slightly smaller than the maximum, its S_{11} is much smaller than that at 25 mm—the curvature radius with maximum gain. Therefore, the optimal curvature radius should be 15 mm.

3.2. Influence of the Position of the Curvature Center of the Semicircle Grooves on the Performance of the Antenna. In the following test, the grooves curvature radius was kept fixed, and the distance between the center of the semicircle and the antenna mouth was adjusted to 28 mm, 30 mm, 32 mm, 34 mm, and 36 mm, respectively. The antennas were simulated using these modified parameters, and the corresponding gain and S_{11} values of the antennas were then measured. The measured gains are presented in Figure 12(a), while the S-parameter measurement results are plotted in Figure 12(b).

From Figure 12, it is evident that when the frequency is 5.8 GHz, the maximum gain is 12.7884 dBi when the center of the semicircle is 32 mm away from the antenna mouth; the minimum gain is 11.7659 dBi when the distance is 36 mm.

At 5.8 GHz with the distance between the center of the semicircle and the antenna mouth at 32 mm, S_{11} is −36.3549, which is the lowest; however, when the distance is 36 mm, S_{11} is −24.977, which is the highest.

The analysis of the numerical results made it possible to identify the performance of the antenna in a complete way. In particular, the curvature radius of the antenna semicircular grooves was found to be 15 mm, while the distance between the curvature center and the antenna mouth was of 32 mm.

3.3. Effect of the Lens on Antenna Performance. A transceiver system consisting of two Vivaldi antennas without and with dielectric lenses was analyzed in order to evaluate their electromagnetic performance. The transverse electric field maps obtained by full-wave numerical simulations are reported in Figure 13.

The component diagram of the transverse electric field obtained from the numerical simulation is shown in Figure 13.

The transmitter signal is 3967 V/m, whereas the signal at the receiver is 1022 V/m with the lens mounted, and 495 V/m without the lens. After the lenses are installed, the waves propagating through the free-space are quite planar, which enhances directivity. Owing to the characteristics of the lens, the microwave energy is more efficiently concentrated, making it easier to collimate into an electromagnetic beam (see Figure 13). After computing the radiation pattern, it is observed that the radiated beam by the lens antenna is only 13.6° at 5.8 GHz, which proves that the antenna exhibits improved characteristics after installing a dielectric lens. The comparative radiation patterns of the antenna without and with the dielectric lens on the main cutting plane are displayed in Figure 14.

The gain measurement results are shown in Figure 15.

A significant improvement in the antenna gain equipped with a dielectric lens is observed in Figure 15. The gain at 5.8 GHz without a lens is 10.46 dBi, whereas the gain at 5.8 GHz with a lens is 16.57 dBi, an increase of 6.11 dBi.

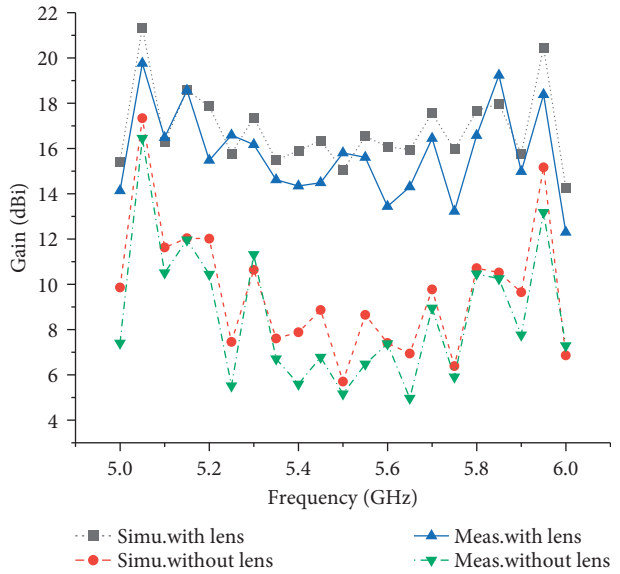

Figure 15: Gain comparison between the antenna without and with a dielectric lens.

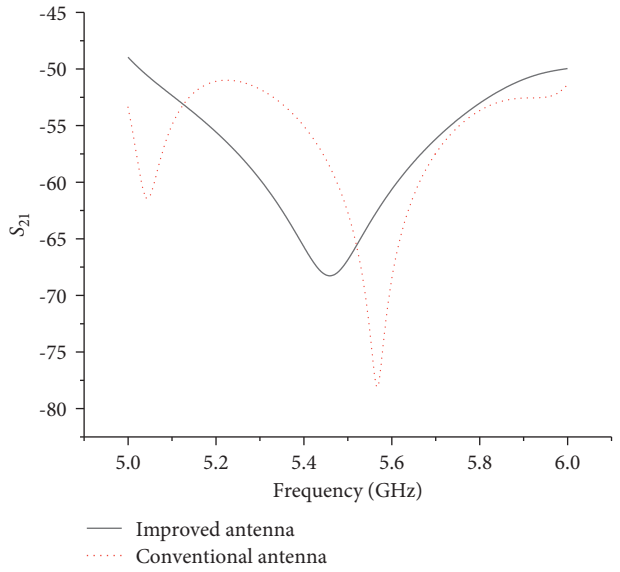

Figure 16: Performance comparison between conventional and improved antenna.

3.4. Antenna Performance Comparison. The humidity measurement system shown in Figure 10 (with and without lens) was simulated numerically using the CST software by assuming water as a device under test. In Figure 16 the computed S_{21} scattering parameters are shown.

From the analysis of the curves shown in Figure 16, it appears that the improved antenna exhibits lower insertion loss than the conventional antenna when the device under test is water, which means that the initial attenuation of the antenna is smaller and the receiving performance are good.

4. Conclusions

Aiming at mitigating the high cost and large volume of traditional horn antennas as well as the deficiencies of conventional Vivaldi antennas (i.e., low gain and poor directivity in low-frequency bands), this paper proposes an affordable and portable Vivaldi lens antenna for grain moisture detection.

Structural parameters affecting antenna performance were compared and analyzed, and it was found that a fence realized on the metal arms can improve antenna gain. The same happens by adding semicircular grooves to the fence structure whose curvature radius and position have a direct impact on the gain. Finally, it was proved that using a dielectric lens a better focusing of electromagnetic waves along the antenna boresight can be achieved, thus significantly increasing the antenna gain.

The antenna is processed and tested successfully; S_{11} is −14.78981 at 5.8 GHz, and the measured results are in good agreement with the numerical simulation. The installation of the lens brings a gain of 6.11 dBi to the antenna. This indicates that the antenna has high gain and good directivity. Premised that this is a printed antenna, its structure is simple, its design is convenient, and its cost is lower than that of the horn antenna, providing a desirable basis for the measurement of grain moisture.

Data Availability

The data used to support the findings of this study are available from the corresponding author upon request.

Conflicts of Interest

The authors declare that there are no conflicts of interest regarding the publication of this paper.

Acknowledgments

This study was supported by the National Natural Science Foundation of China (32071911), Shandong Modern Agricultural Industry System Wheat Industry Innovation Team (SDIT-01-12), and the Qingdao Agricultural University Doctoral Start-Up Fund (1119049).

References

[1] S. Jiarasuwan, K. Chamnongthai, and N. Kittiamornkul, "A design method for a microwave-based moisture sensing system for granular materials in arbitrarily shaped containers," *IEEE Sensors Journal*, vol. 21, no. 17, pp. 19436–19452, 2021.

[2] C. Zhang, Z. Shi, H. Yang, X. Zhou, Z. Wu, and D. S. Jayas, "A novel, portable and fast moisture content measuring method for grains based on an ultra-wideband (UWB) radar module and the mode matching method," *Sensors*, vol. 19, no. 19, p. 4224, 2019.

[3] S. Trabelsi, M. A. Lewis, and S. O. Nelson, "Microwave moisture meter for in-shell peanut kernels," *Food Control*, vol. 66, pp. 283–290, 2016.

[4] A. Hatami, A. Saee Arezomand, and F. B. Zarrabi, "Phase center controlling in Vivaldi antenna: review and development of the story," *Journal of Computational Electronics*, vol. 19, no. 2, pp. 736–749, 2020.

[5] S. Saleh, W. Ismail, I. S. Z. Abidin, M. H. Jamaluddin, M. H. Bataineh, and A. S. Alzoubi, "Compact UWB Vivaldi tapered slot antenna," *Alexandria Engineering Journal*, vol. 61, no. 6, pp. 4977–4994, 2022.

[6] F. Lin, Y. Qi, J. Fan, and Y.-C. Jiao, "0.7–20-GHz dual-polarized bilateral tapered slot antenna for EMC measurements," *IEEE Transactions on Electromagnetic Compatibility*, vol. 56, no. 6, pp. 1271–1275, 2014.

[7] G. Teni, N. Zhang, J. Qiu, and P. Zhang, "Research on a novel miniaturized antipodal Vivaldi antenna with improved radiation," *Antennas Wirel. Propag. Lett.,* vol. 12, pp. 417–420, 2013.

[8] M. T. Islam, M. Z. Mahmud, N. Misran, J.-I. Takada, and M. Cho, "Microwave breast phantom measurement system with compact side slotted directional antenna," *IEEE Access*, vol. 5, pp. 5321–5330, 2017.

[9] R. Xu, S. Gao, B. S. Izquierdo et al., "A review of broadband low-cost and high-gain low-terahertz antennas for wireless communications applications," *IEEE Access*, vol. 8, pp. 57615–57629, 2020.

[10] H. M. A. Rahman, M. M. Khan, M. Baz, M. Masud, and M. A. AlZain, "Novel compact design and investigation of a super wideband millimeter wave antenna for body-centric communications," *International Journal of Antennas and Propagation*, vol. 2021, Article ID 8725263, 15 pages, 2021.

[11] D. Chen, K. Wang, W. Zhu et al., "2–40 GHz dual-band dual-polarised nested Vivaldi antenna," *IET Microwaves, Antennas & Propagation*, vol. 13, no. 2, pp. 163–170, 2019.

[12] T. Nahar and S. Rawat, "Survey of various bandwidth enhancement techniques used for 5G antennas," *International Journal of Microwave and Wireless Technologies*, vol. 14, no. 2, pp. 204–224, 2022.

[13] O. Ari and A. Kizilay, "Broadband all-metal Vivaldi antenna with Rexolite inserted slot edge," *Microwave and Optical Technology Letters*, vol. 64, no. 4, pp. 778–788, 2022.

[14] J. Shin and D. H. Schaubert, "A parameter study of stripline-fed Vivaldi notch-antenna arrays," *IEEE Transactions on Antennas and Propagation*, vol. 47, no. 5, pp. 879–886, 1999.

[15] Y. Cao, G. A. E. Vandenbosch, and S. Yan, "Low-profile dual-polarized multi-beam antenna based on pillbox reflector and 3D-printed ridged waveguide," *IEEE Transactions on Antennas and Propagation*, p. 1, 2022.

[16] J. Eichenberger, E. Yetisir, and N. Ghalichechian, "High-gain antipodal Vivaldi antenna with pseudoelement and notched tapered slot operating at (2.5 to 57) GHz," *IEEE Transactions on Antennas and Propagation*, vol. 67, no. 7, pp. 4357–4366, 2019.

[17] D. Schaubert, E. Kollberg, T. Korzeniowski, T. Thungren, J. Johansson, and K. Yngvesson, "Endfire tapered slot antennas on dielectric substrates," *IEEE Transactions on Antennas and Propagation*, vol. 33, no. 12, pp. 1392–1400, 1985.

[18] H. Hijazi, M. Le Roy, R. Lababidi, D. Le Jeune, and A. Pérennec, "Ultra-wideband antenna system for in-band full-duplex applications," *IET Microwaves, Antennas & Propagation*, vol. 15, no. 15, pp. 1853–1865, 2021.

[19] V. Binzlekar, A. Sharma, and S. Agarwal, "A high gain and wide bandwidth Grooved AML loaded Vivaldi Antenna design for imaging and communication applications," *Microwave and Optical Technology Letters*, vol. 64, no. 7, pp. 1217–1223, 2022.

[20] R. Cicchetti, V. Cicchetti, A. Faraone, L. Foged, and O. Testa, "A compact high-gain wideband lens Vivaldi antenna for wireless communications and through-the-wall imaging," *IEEE Transactions on Antennas and Propagation*, vol. 69, no. 6, pp. 3177–3192, 2021.

[21] G. K. Pandey, H. S. Singh, P. K. Bharti, A. Pandey, and M. K. Meshram, "High gain Vivaldi antenna for radar and microwave imaging applications," *IJSPS*, vol. 3, 1 page, 2014.

[22] G. Zhu, Y. Ding, and G. Yang, "Design of shaped dielectric lens antenna for millimeter wave wind profile radar," in *Proceedings of the 2021 International Conference on Microwave and Millimeter Wave Technology (ICMMT)*, pp. 1–3, Nanjing, China, May 2021.

[23] J. C. Valencia-Estrada, R. B. Flores-Hernández, and D. Malacara-Hernández, "Singlet lenses free of all orders of spherical aberration," *Proceedings of the Royal Society A: Mathematical, Physical & Engineering Sciences*, vol. 471, no. 2175, Article ID 20140608, 2015.